Sensitized and Intrinsic In-Plane Photocurrents in Langmuir−Blodgett Films of 7-(2-Anthryl)-1-heptanoic Acid

A. Vaes, M. Van der Auweraer,*,[1] P. Bosmans, and F. C. De Schryver

Laboratory of Photochemistry and Spectroscopy, Katholieke Universiteit, Leuven, Celestijnenlaan 200 F, B-3001 Heverlee, Belgium

Received: December 31, 1997; In Final Form: April 8, 1998

Langmuir−Blodgett (LB) films of an amphiphilic long-chain derivative of anthracene, of which the molecular packing shows a strong resemblance with the *ab*-plane of anthracene crystals, were investigated with respect to their photoconductive properties. Efficient photoinduced charge carrier generation and in-plane charge transport have been observed in LB-films of (2A7), using a gap configuration. The wavelength and intensity dependence of the quantum yield of the photocurrent in absence of a photosensitizer suggest an intrinsic bulkcharge generation mechanism. The intensity dependence of the photocurrent suggests a combination of nongeminate and alien recombination of charge carriers. The increase of the quantum yield in the presence of air is an indication that, upon photoexcitation, mobile holes are formed. By covering the multilayer assembly with a rhodamine containing monolayer, a significant increase of the quantum yield is obtained upon excitation of both the anthracene chromophore and the dye. In the case of dye excitation, the values and the field dependence of the photocurrents due to the photosensitized injection of holes from the layer of excited dye molecules into the 2A7 multilayer resemble those obtained for anthracene crystals covered by adsorbed dyes.

1. Introduction

The photoconductive properties of anthracene single crystals, both intrinsic and sensitized, have been investigated extensively in the past. The intrinsic charge generation and transport mechanism of anthracene single crystals have been discussed.[2,3] Photosensitized hole injection into anthracene crystals has been studied by covering the crystals with adsorbed cationic dyes or dye monolayer assemblies.[4,5] At low dye coverages and at sufficiently high electrical fields, quantum yields up to 100% have been reported.[6,7]

During the last years, interest the photoconductive properties of Langmuir−Blodgett (LB) films has an increased, based on the possibility to construct molecular architectures that allow the study of physical phenomena on a molecular level. Practical interest arises from the continuous trend of size reduction of electronic devices. While until now most investigations of photocurrents in LB-films were focused on photoconduction across the monolayers,[8,9] less attention has been paid to the observation of lateral transport parallel to the monolayer interface. Donovan et al.[10,11] studied transient photocurrents in the plane of polydiacetylene multilayers. Roberts et al.[12] showed that there is a marked anisotropy in the conductivity of 9,10-substituted anthracene LB-films. Sugi et al.[13−14] studied anisotropic photoconduction in dye sensitized Langmuir films upon incorporating surface active merocyanine dyes in a fatty acid matrix.

In the present contribution, we report the photoconductive properties of a surface active anthracene derivative (2A7) (Figure 1) incorporated in an anisotropic LB-film, where the packing of the anthracene moieties is similar to that in the *ab*-plane of anthracenes.[15] 2A7 has been used earlier to interface a cyanine dye containing monolayer and an anthracene crystal.[16−17] The molecular packing of 2A7 multilayers, where the short axis of the anthracene moiety is in the plane of the monolayer and where

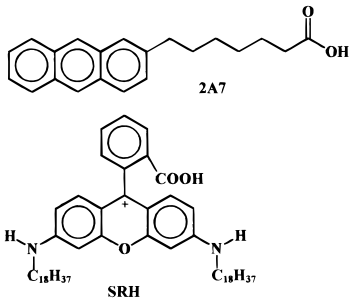

Figure 1. The chemical structures of 2A7 and SRH.

the long axis is nearly parallel to the normal on the monolayer plane,[26] is expected to favor charge transport parallel to the substratum. It is our aim to investigate to which extent the photoconductivity, observed for anthracene single crystals, can be extrapolated to LB-films of 2A7. In a first step, information was obtained about the charge generation and recombination mechanism of nonsensitized in-plane photocurrents upon variation of several experimental parameters. In a second step, the generation of photosensitized hole currents in the 2A7 multilayer was investigated. For this purpose, mixed monolayers of N,N′-bis(stearyl)-rhodamine B (SRH) (Figure 1) and arachidic acid (AA) were deposited on top of the 2A7 multilayers. The former experiment has, to our knowledge, not been performed earlier on Langmuir−Blodgett films of this type. We will extend the results obtained for anthracene crystals to the amphiphilic anthracene derivative 2A7.

2. Experimental Section

2A7 has been prepared according to Kaplun et al.[18] Arachidic acid (AA) (Janssen) was used without further purification. SRH has been prepared according to Ioffe et al.[19]

In the pressure area diagrams of a monolayer of 2A7 on a subphase of 5×10^{-4} M $CdCl_2$ in milli-Q at pH 4.8, determined

S1089-5647(98)00613-0 CCC: $15.00
Published on Web 06/20/1998

using a KSV5000 ALT trough, the onset of the compression is observed at a molecular area of 29 Å^2/molecule. The collapse pressure of a monolayer of 2A7 is 50 mN/m at a molecular area of 23 Å^2/molecule. This is in agreement with the results of Durfee[26] and Biesmans.[20] Multilayers of 2A7 were prepared at a surface pressure of 22 mN/m and deposited at a rate of 5 mm/min. Cospreading of SRH and AA on a 5×10^{-4} M solution of $CdCl_2$ in milli-Q at pH 5.5 allowed us to obtain mixed monolayers. These monolayers could be deposited with a rate of 5 mm/min on quartz at a surface pressure of 30 mN/m. Two different mixed monolayers were prepared, in which the mole ratio SRH/AA was 1:100 and 1:10, respectively.

Absorption spectra of the multilayer assemblies were measured with a Perkin-Elmer Lambda-6 spectrophotometer. Corrected emission spectra were obtained with a SPEX Fluorolog, using front face excitation. To avoid quenching by O_2 and photooxidation, the fluorescence spectra of the multilayer assemblies were determined at reduced pressure (0.1 mbar).

Because the molecular structure of 2A7 multilayers is expected to favor charge transport parallel to the substratum, the photocurrents were investigated using a gap configuration,[21] described elsewhere.[22] A second reason for the use of such a gap configuration, instead of a more common sandwich configuration, is that the currents normal to Langmuir−Blodgett films, sandwiched between two metal electrodes, can be biased by the occurrence of short circuits at pinholes.[23] In the first step, an array of interdigitated aluminum electrodes was evaporated on a quartz slide, cleaned using the procedures described elsewhere.[24] In the next step, the substrates were covered by up to 20 layers of 2A7 or 19 layers of 2A7 and a monolayer of arachidic acid containing the dye. Except when indicated otherwise, the results of the photocurrents refer to data obtained at reduced pressure (0.1 mbar), at room temperature, and using aluminum electrodes with a spacing of 100 μm. The electrodes were brought in contact by brass springs and mounted in a sample holder that could be evacuated to reduced pressure.

For the measurement of the stationary photocurrents, a Kepco OPS 2000 amplifier and a triangular wave generator were applied to the electrode array, yielding a field strength up to 1.0×10^7 V/m. The currents were determined using a Keithley 610C electrometer. Due to a protection circuit[27] of the entrance of the electrometer, the response time of the setup amounts to several seconds. For the determination of the photocurrents, the sample was illuminated by a 1500 W xenon lamp (Schöffel GmbH) via a heat filter and a monochromator (Applied Photophysics, Ltd., High Radiance Monochromator). The intensity was determined using an IL1700 Research Radiometer from International Light, Inc., with a Sed400 probe. The current voltage plots or the action spectra of the photocurrent were obtained in a discontinuous way: for each data point, the applied voltage or the wavelength of the monochromator was set to the appropriate value and the current was allowed to relax to a stationary value during 10 to thirty seconds. At reduced pressure, voltages between 0 and 400 V could be applied, yielding electric fields between 0 and 4.0×10^4 V/cm. At higher applied voltages, dielectric breakdown, indicated by the observation of sparks and large spurious transient currents, occurred. In air, no dielectric breakdown occurred below 1000 V. This points to that the dielectric breakdown is connected to the process of thermionic emission from the metal electrodes. Except when indicated otherwise, the $i-V$ plots were recorded upon increasing the applied field.

The knowledge of the optical density, the photocurrent, and the incident intensity allows the calculation of the quantum yield

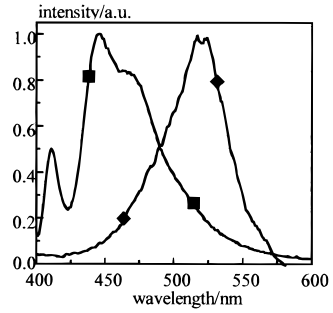

Figure 2. Emission spectrum ($\lambda_{ex} = 385$ nm) of a 20 layer LB-film of 2A7 and absorption spectrum of a mixed monolayer of SRH in AA (AA/SRH = 10:1). The spectra are normalized at the maximum.

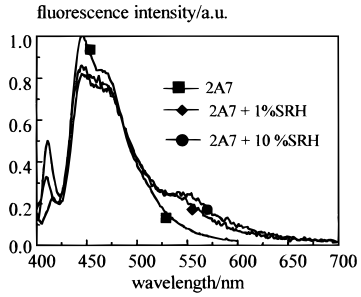

Figure 3. Emission spectra ($\lambda_{ex} = 385$ nm) of a 20 layer LB-film of 2A7, an LB-film of 2A7 + a monolayer of 1% SRH in AA, and a LB-film of 2A7 + a monolayer of 10% SRH in AA.

of the stationary photocurrent ϕ_{st}, using

$$f_{st} = \frac{1.238 \times 10^3 i_{st}}{I_0 \lambda_{ex}(1 - 10^{-Abs})S} \quad (1)$$

In eq 1 I_0, Abs, λ_{ex}, i_{st}, and S correspond to the incident light intensity in W/m^2, the absorbance of the sample at the excitation wavelength, the excitation wavelength in nm, the observed photocurrent in A, and the illuminated area of the Langmuir−Blodgett film between the metal electrodes (5.4×10^{-9} m^2), respectively.

3. Results

3.1. Energy Transfer between 2A7 and SRH. The spectroscopic properties of LB-films of 2A7 have been reported previously.[26,32,37] To discuss the mechanism of sensitized hole injection observed for a 2A7 multilayer covered with a SRH monolayer (vide infra), however, it is necessary to investigate the possible occurrence of energy transfer between 2A7 and SRH. The good overlap between the 2A7 fluorescence spectrum and the SRH absorption spectrum (Figure 2) suggests that this process could be efficient. Because the absorption and emission bands of both compounds are well separated, stationary fluorescence measurements allow the evaluation of the efficiency of the energy transfer.

In Figure 3, emission spectra are shown for a pure 2A7 multilayer and a multilayer of 2A7 covered with a mixed monolayer of SRH (1% and 10%, respectively) in AA for selective excitation of 2A7 (385 nm). Two emission bands are observed when the multilayer of 2A7 is covered with a mixed multilayer of SRH: the one at shorter wavelengths corresponds to 2A7 fluorescence,[32] while that at longer wavelengths is due to photosensitized fluorescence of SRH.[26] The band at low energies is broader for the sample in which the SRH concentration is 10%. These experiments show that the fluorescence intensity of 2A7, covered by a 1% or 10% SRH monolayer,

differs less than 20% of the fluorescence intensity of 2A7 in the absence of an SRH monolayer. This means that, despite the good spectral overlap, energy transfer from 2A7 to SRH is a relative inefficient process. One of the reasons could be the low fluorescence quantum yield of 2A7 in undiluted LB-films. The quantum yield of a undiluted 2A7 monolayer was determined to be 10^{-2} by Verschuere et al.[37] This will reduce the value of R_0 for both direct energy transfer from 2A7 to SRH and hopping of excitation between the different 2A7 layers. Furthermore, only the upper layers of 2A7 will be close enough to the SRH layers to be able to transfer their excitation energy efficiently. This means that for a sample containing 20 2A7 layers, only 10% can transfer energy to the SRH layer if no efficient energy hopping between 2A7 double layers, which are separated by 36 Å, occurs.

3.2. Nonsensitized In-Plane Photocurrents in LB-Films of 2A7. When a potential difference of 100 V (1.0×10^4 V/cm) is applied on an interdigitating aluminum electrode covered by 20 layers of 2A7 at reduced pressure (0.1 mbar), a dark conductivity σ of 7.4×10^{-14} S/cm is observed, which is typical for insulating systems. At reduced pressure the dark current is for the experimentally accessible range of field strengths (5−45 kV/cm) proportional to the square of applied field. It is increased by 1 order of magnitude at atmospheric pressure. This non-Ohmic behavior would suggest that the dark current is either injection or space charge limited. The dark conductivity of the multilayers of 2A7 resembles that of anthracene crystals.[27] Using aluminum electrodes, the dark current density of multilayers of 2A7 amounts to 7.4×10^{-6} A/m^2 at an applied field of 1.0×10^6 V/m. These current densities are 5 orders of magnitude smaller than those obtained for multilayers of 9-butyl-10-anthrylpropanoic acid[22] in the plane of the Langmuir−Blodgett film at a field strength of 1.0×10^6 V/m using Al electrodes, and 2 orders of magnitude smaller than observed perpendicular to the film at a field strength of 1.0×10^6 V/m. The dark conductivity of multilayers of 2A7 is several orders of magnitude smaller than that of LB-films of unsubstituted metal-free phthalocyanine, where a value of 2.6×10^{-9} S/cm was obtained.[28] This is probably due to the larger band gap and/or higher ionization potential of 2A7. The rise or decay times of the photocurrent observed upon starting or stopping the illumination correspond to those obtained when changing the applied voltage over a large Ohmic test resistor. This suggests that the observed response time of the sample is faster than that of our setup.

Excitation at 400 nm (9.9 W/m^2) yields a photocurrent of 3.4×10^{-10} A (0.1 mbar) at an applied field of 1.0×10^4 V/cm. This corresponds to a quantum yield of 6.7×10^{-5}. At reduced pressure, the photocurrent and the quantum yield show a linear dependence on the applied field (Figure 4). At atmospheric pressure the photocurrent is 15−30 times larger than at the reduced pressure. In the current versus voltage plot, two linear regimes can be distinguished: Above 600 V, the photocurrent increases more rapidly with the electrical field than at low fields. At an applied field of 4.0×10^4 V/cm, the photocurrent and the quantum yield amount to 2.4×10^{-8} A and 4.7×10^{-3}, respectively (Table 1).

From the influence of the light intensity and the wavelength on the photocurrent and its quantum yield ϕ_{st}, information is obtained about the generation and recombination of the charge carriers. Upon excitation at 400 nm, both under atmospheric pressure and at reduced pressure, the photocurrent shows a power law dependence on the intensity of the incident light, $i = I^m$, where $m \approx 0.75$ (Figure 5). The quantum yield decreases

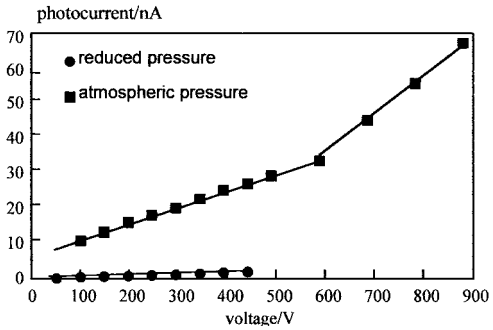

Figure 4. Influence of the voltage on the photocurrent for an aluminum electrode covered by 20 layers of 2A7 at reduced pressure and at ambient atmosphere. Excitation occurred at 400 nm (9.9 W/m^2).

TABLE 1: Quantum Yields of the Stationary Photocurrents. The Applied Voltage Was 400 V (4.0×10^4 V/cm)

sample	$\phi_{vac}{}^a$	$\phi_{O2}{}^a$	$\phi_{vac}{}^b$	$\phi_{O2}{}^b$
20 layers 2A7	3.1×10^{-4}	4.7×10^{-3}		
19 layers 2A7 + 1 layer SRH (1%)	5.4×10^{-3}	3.6×10^{-2}	4.3×10^{-3}	1.0×10^{-2}
19 layers 2A7 + 1 layer SRH (10%)	1.7×10^{-3}	1.7×10^{-2}	1.1×10^{-3}	5.6×10^{-3}

^{a} $\lambda_{ex} = 400$ nm. ^{b} $\lambda_{ex} = 530$ nm.

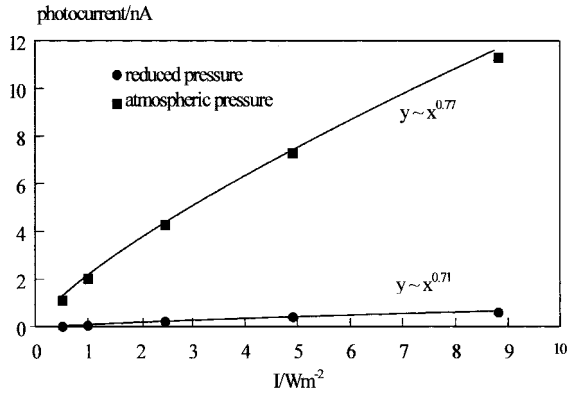

Figure 5. Influence of the incident light intensity on the photocurrent quantum yield ϕ_{st} for an aluminum electrode covered by 20 layers of 2A7 at reduced pressure and at atmospheric pressure. The applied field was 2.0×10^4 V/cm, and the excitation wavelength was 400 nm.

TABLE 2: Intensity Dependence of the Stationary Photocurrent Quantum Yields ($\phi_{st} \sim I^\gamma$). Applied Voltage Was 200 V (2.0×10^4 V/cm)

sample	$\gamma_{vac}{}^a$	$\gamma_{O2}{}^a$	$\gamma_{vac}{}^b$	$\gamma_{O2}{}^b$
20 layers 2A7	−0.29	−0.23		
19 layers 2A7 + 1 layer SRH (1%)	−0.08	−0.14	−0.01	−0.06
19 layers 2A7 + 1 layer SRH (10%)	−0.19	−0.29	−0.05	−0.02

^{a} $\lambda_{ex} = 400$ nm. ^{b} $\lambda_{ex} = 530$ nm.

upon increasing the incident light intensity up to 10 W/m^2. When the intensity dependence of ϕ_{st} is approximated by the power law $\phi_{st} \sim I^\gamma$, a value between $-1/2$ and 0 is obtained for γ (Table 2).

Upon changing the excitation wavelength, a photocurrent action spectrum is obtained with a maximum at 397 nm (Figure 6a), which is close to the absorption maximum (situated at 401 nm). Taking into account the duration of this experiment, the action spectrum has been recorded only at reduced pressure to avoid photooxidation effects. Such photooxidation effects have been observed for poly(*N*-vinylcarbazole)[29] and triphenylene derivatives[34,42] upon prolonged illumination. Despite the resemblance between the action spectrum and the absorption spectrum of a multilayer of 2A7, the quantum yield depends

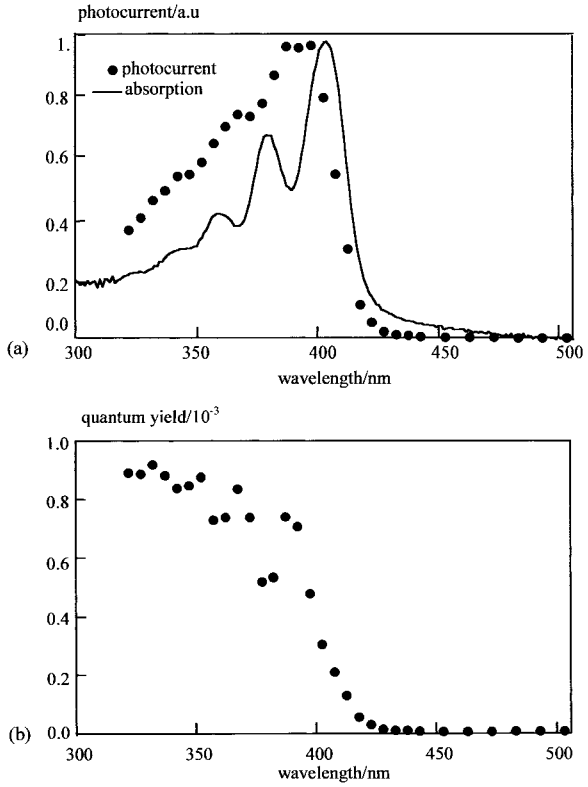

Figure 6. Photocurrent action spectrum (a) and influence of the wavelength on the quantum yield (b) for an aluminum electrode covered by 20 layers of 2A7, both at reduced pressure. The applied field was 4.0×10^4 V/cm. The absorption spectrum and action spectrum are normalized at the maximum.

on the wavelength of excitation (Figure 6b). Upon decreasing the wavelength of the excited light, an increase of the quantum yield is observed, which levels off below 350 nm. At 330 nm (3.73 eV), the quantum yield is 9.3×10^{-4}. The charge carriers are most efficiently generated in the region below 350 nm. At wavelengths exceeding 385 nm the quantum yield starts to decrease rapidly.

3.3. Photosensitized Photocurrents in LB-Films of 2A7. Deposition of a mixed monolayer of SRH in AA on top of a multilayer of 2A7 allows to obtain sensitized hole currents (SHC). In agreement with the observation for a multilayer of 2A7 not covered with a dye monolayer, a maximum of the photosensitized photocurrent is obtained around 400 nm for both the 1% and the 10% samples (Figure 7). For the 10% sample one also clearly observes a photocurrent upon excitation of the dye chromophore in the range between 500 and 540 nm. For the 1% sample, which has a lower absorbance in this region, this sensitized photocurrent is less important. With the dye layer, excitation at either 400 or 530 nm leads to a significant increase of the quantum yield in comparison with corresponding nonsensitized systems. In both cases, the concentration of SRH clearly influences the SHC. The highest quantum yields are obtained when a 1% SRH monolayer is deposited on top of the 2A7 multilayer (Table 1).

3.3.1. Excitation at 530 nm. This experiment resembles the photosensitization experiments that have been performed on anthracene crystals covered with cationic dyes.[10−13,27−29] At reduced pressure, the photocurrent at 530 nm increases linearly with the applied field at low fields but levels off at higher fields (Figure 8). This effect is more pronounced for the 10% sample compared to the 1% sample. Recording the current versus voltage plot a second time upon decreasing the applied field

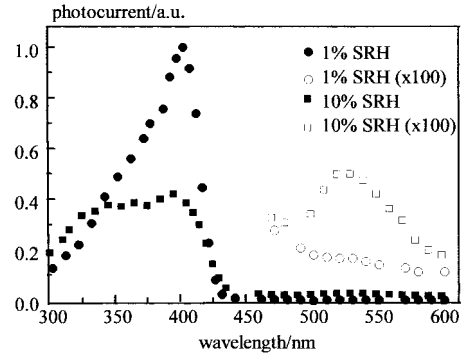

Figure 7. Influence of the wavelength on the photocurrent at reduced pressure for an aluminum electrode covered by 19 layers of 2A7 and a monolayer of SRH in AA. The concentration of SRH in AA amounted to 1% and 10%. The applied field equalled 4.0×10^4 V/cm. For the photocurrent a correction has been made for the wavelength dependence of the incident intensity.

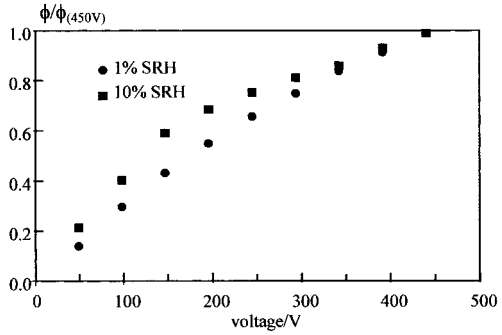

Figure 8. Influence of the applied voltage at reduced pressure on the relative quantum yield of the photosensitized photocurrent for an aluminum electrode covered by 19 layers of 2A7 and a monolayer of SRH in AA. The concentration of SRH in AA was 1% and 10%. Excitation occurred at 530 nm (10.4 W/m^2). All quantum yields are normalized to the quantum yield at 450 V.

yields values for the SHC that are about 5% lower than the values of the first cycle (Figure 9). This cannot be due to a neglect of the capacitive currents, as the photocurrents are 4 orders of magnitude higher than the dark currents. These dark currents should also be perturbed by the capacitive currents, which is evidently not the case.

In the presence of air the SHC is enhanced. The quantum yields at atmospheric pressure are a factor 3−5 larger than the corresponding values at reduced pressure (Table 1). At atmospheric pressure, a very fast initial rise (Figure 9b) is followed by a linear increase of the photocurrent up to a potential of 400 V. Above 400 V a superlinear increase is observed (Figure 9a). In contrast to what was observed at reduced pressure, the values of the photocurrents recorded during the second cycle are about 20 à 25% higher than the values recorded during the first cycle.

The dependence of the SHC at 530 nm on the light intensity differs substantially from the behavior of the nonsensitized photocurrents obtained at 400 nm. In both samples (1% and 10%), the photocurrent is proportional with the light intensity (Figure 10), and the quantum yield is independent of the light intensity ($\gamma \approx 0$) (Table 2).

3.3.2. Excitation at 400 nm. Upon excitation of the anthracene chromophore, the quantum yields obtained for the 1% and the 10% sample are a factor 18 and 5, respectively, larger than the corresponding values obtained for a 20 layer 2A7 film not sensitized by SRH. The voltage dependence is identical to the dependence observed for multilayers of 2A7 without a dye

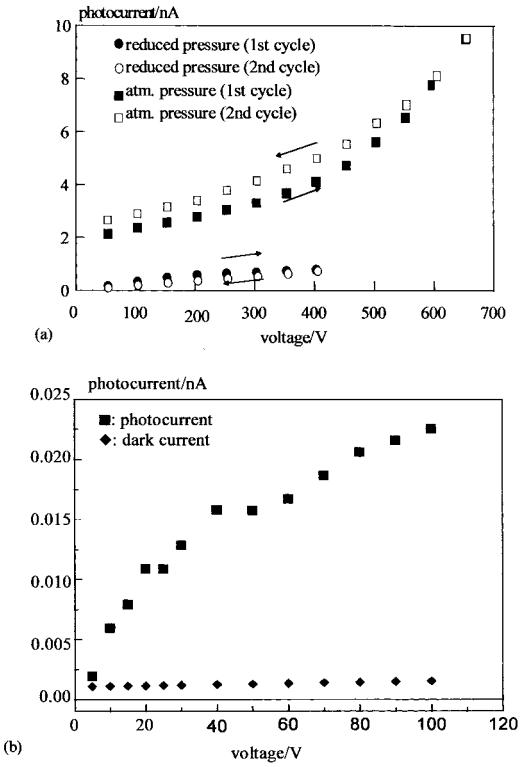

Figure 9. Influence of the applied voltage on the photosensitized photocurrent for an aluminum electrode covered by a multilayer of 2A7 and a monolayer of SRH in AA. Excitation occurred at 530 nm (10.4 W/m^2). (a) The hole transport layer consisted of 19 layers of 2A7. The sensitizing layer contained 10% SRH in AA and the excitation intensity amounted to 10.4 W/m^2. The photocurrent was determined at reduced pressure and at atmospheric pressure. During the first cycle, the applied field was increased, whereas during the second cycle, it was decreased. (b) The hole transport layer consisted of 12 layers of 2A7. The sensitizing layer contained 1.5% SRH in AA, and the excitation intensity amounted to 7.3 W/m^2. The photocurrent was obtained at atmospheric pressure

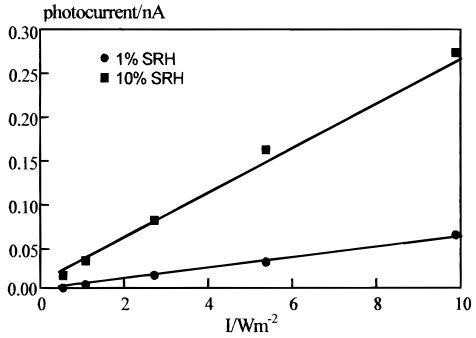

Figure 10. Influence of the incident light intensity at reduced pressure on the photocurrent quantum yield ϕ_{st} for an aluminum electrode covered by 19 layers of 2A7 and a monolayer of SRH in AA. The concentration of SRH in AA amounted to 1% and 10%. The applied field amounted to 2.0×10^4 V/cm. Excitation occurred at 530 nm.

monolayer on top. Upon introduction of air, the quantum yield at 400 nm is increased further by about 1 order of magnitude. The enhancement of the quantum yield of the SHC in the presence of air is more important at 400 nm than at 530 nm.

In contrast to what was observed upon excitation at 530 nm, the SHC obtained at 400 nm is not proportional to the light intensity and the quantum yield shows a small dependence on the light intensity (Table 2). The values of γ are closer to those obtained for multilayers of 2A7 upon excitation at 400 nm than to the values obtained for multilayers of 2A7 covered with SRH upon excitation at 530 nm.

4. Discussion

4.1. Nonsensitized In-Plane Photocurrents in Multilayers of 2A7. *4.1.1. Generation and Recombination Mechanism.* Excitation of a sample consisting of an aluminum electrode covered by twenty layers of 2A7 at 400 nm yields a photocurrent, which is 4 orders of magnitude larger than the dark current at the same applied potential. Quantum yields ($10^{-5}-10^{-4}$) at reduced pressure agree with the values of the intrinsic photoinduced production of electron−hole pairs in anthracene crystals, while the quantum yields ($10^{-3}-10^{-2}$) at atmospheric pressure more closely resemble the values found for exciton dissociation at the surface of anthracene crystals.[31] The light intensity dependence of the quantum yield and the photocurrent suggest that, both in the presence and absence of oxygen, nongeminate recombination is an important although not exclusive mechanism for the charge carrier recombination. In the case of nongeminate recombination the hole and the electron are due to the absorption of two different photons. This means that besides nongeminate recombination, alien recombination, deep trapping, or neutralization of the charge carriers at the opposite electrode must be important, otherwise, γ would be -0.5. To which extent geminate recombination of an electron−hole pair is important cannot be determined from the intensity dependence of the photocurrent. In the case of geminate recombination the hole and the electron are due to the absorption of the same photon. The dependence of the photocurrent and the quantum yield on the intensity is similar to the behavior observed for the photocurrent in the plane of multilayers of triphenylene derivatives[42] and for the photocurrent in the plane of mixed multilayers of cadmium arachidate and a merocyanine dye.[23]

Nongeminate recombination implies that charge carriers of both polarities are generated in the bulk of the multilayer assembly and not by the dissociation of an exciton. Also the rapid trapping of one type of charge carriers, leading to the formation of recombination centers for charge carriers of opposite sign, can cause nongeminate recombination. The increase of the quantum yield below 380 nm is compatible with an intrinsic mechanism, yielding electron−hole pairs. Upon decreasing the excitation wavelength, either the efficiency of the primary photoionization or the separation between the electron and the hole in the initial geminate pair will increase,[32,33] leading to a larger photocurrent. On the other hand, if the charge carriers would be generated by transport of a mobile exciton to the interface, where interaction with the electrode or an impurity would lead to mobile holes, there is no reason to assume that this process will become more efficient upon excitation at shorter wavelengths. The influence of the wavelength on the quantum yield suggests that the Onsager model[34] can be used to describe the charge generation mechanism. The photocurrent levels off at a photon energy of 3.7 eV, which is 0.2 eV below the generally accepted value for the band gap (3.9 eV) in anthracene crystals.[35,36] The increase of the quantum yield upon increasing the applied field is due to a more efficient dissociation of electron−hole pairs or to an increase of the Schubweg (the characteristic distance the charge carriers move in the material before being trapped in a deep trap or annihilating through carrier recombination).

It should be remarked that the onset of the action spectrum is slightly blue shifted in comparison with the absorption spectrum. The way the photocurrent action spectra are obtained excludes that this effect is due to a delayed response of the

photocurrent on the change of the wavelength of the excitation light. The effect may, however, be due to an instrumental effect, as the bandwidth of the slits used will lead to a convolution with the actual action spectrum. A second, more fundamental explanation is the possible occurrence of a strong inhomogenity of the absorption band. Excitation of low lying excited states at longer wavelengths leads to excitons that dissociate less easily to electron−hole pairs. Furthermore, the low energy excitons produced by long wavelength excitation are expected to be to a lesser extent involved in energy migration to a site where dissociation of the exciton could be favored.

4.2.2. Influence of Air. The photocurrent is increased by a factor of fifteen to thirty at atmosphere pressure as compared to reduced pressure. This implies that the photocurrent is not due to the photogeneration of mobile electrons. The increase of ϕ_{st} can be due to several processes involving oxygen: (a) an increase of the generation efficiency η. The increase of the photocurrent upon the admission of air suggests that photocurrents are generated by the interaction between excitons and oxygen, leading to the formation of mobile holes and superoxide anions (eq 3). However, the intensity dependence in the presence of air indicates that the radical anions must be adsorbed at or in the sample at sites where they still can recombine with the mobile holes.

$$(AA)^* \xrightarrow{E} A^{+\bullet} + A^{-\bullet} \text{ without oxygen} \quad (2)$$

$$(AA)^* \xrightarrow{E_2O_2} A^{+\bullet} + A + O_2^{-\bullet} \text{ with oxygen} \quad (3)$$

(b) Intrinsic formation of electron−hole pairs, followed by a capture of the mobile electrons by oxygen (eq 4). In analogy to the first mechanism, this mechanism will only lead to an important increase of the photocurrent, if recombination between the superoxide molecules and the mobile holes is slowed significantly. If the recombination is completely blocked, the photocurrent would depend in a linear way on the intensity, contrary to our observations.

$$(AA)^* \xrightarrow{E} A^{+\bullet} + A^{-\bullet} \xrightarrow{O_2} A^{+\bullet} + A + O_2^{-\bullet} \text{ with oxygen} \quad (4)$$

4.2. Photosensitized Photoconductivity in Multilayers of 2A7 Covered with a Monolayer of SRH in AA. Exciting either the dye monolayer (D) or the 2A7 multilayer (A) yields a photosensitized photocurrent. Because of the similarity with sensitized injection of adsorbed dyes into anthracene crystals, the experimental data will be discussed in the framework of the model developped for the latter system (see Scheme 1).

SCHEME 1: Redox Levels of SRH, SRB, and 2A7

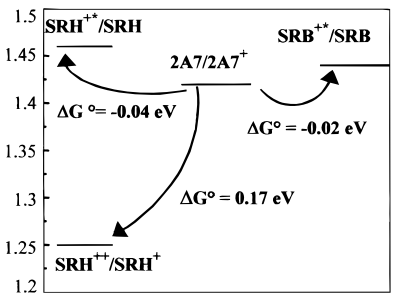

4.2.1. Excitation at 530 nm. Mechanism of Photosensitized Charge Generation. For the photosensitized current obtained upon excitation at 530 nm, the following mechanism, which was established for dye molecules adsorbed on anthracene crystals,[12,13,49] can be proposed.

TABLE 3: Parameters of the Charge Injection Process

system	$E_{D/D-}$/eV	E_{00D}/eV	$E_{D*/D-}$/eV	$\Delta G°$/eV
SRH-2A7	−0.83	2.29	1.46	−0.04
SRB-2A7[51]	−0.75	2.19	1.44	−0.02
oxacarbocyanine-2A7[28]	−1.04	2.49	1.45	−0.03

$$D + A \xrightarrow{h\nu} {}^1D^* + A \qquad \text{excitation: } 450 < \lambda < 550 \text{ nm} \quad (5)$$

This step is followed by several competitive processes:

$${}^1D^* \rightarrow D + h\nu_D \qquad \text{fluorescence} \quad (6)$$

$${}^1D^* \rightarrow D \qquad \text{radiationless decay processes} \quad (7)$$

$${}^1D^* + A \rightarrow D^{-\bullet} + A^{+\bullet} \qquad \text{charge transfer quenching} \quad (8)$$

$$D^{-\bullet} + A^{+\bullet} \xrightarrow{E} D^{-\bullet} + A + h^{+\bullet} \qquad \text{field-assisted charge separation} \quad (9)$$

$$D^{-\bullet} + A^{+\bullet} \rightarrow D + A \qquad \text{geminate recombination} \quad (10)$$

In this framework, the adsorbed dye can be considered as a primary electron acceptor (eq 8). Excitation of the dye leads to injection of a hole into the first layer of the aromatic single crystal or 2A7 multilayer. Considering that the ionization potentials of 2-alkylanthracenes are equal to that of anthracene and that the polarizability of a monolayer is close to that of an anthracene crystal, a value of 1.42 V can be assumed for the oxidation potential ($E_{A+/A}$) of the upper layer of a 2A7 multilayer.[28] The reduction potential ($E_{D/D-}$) of SRH is −0.83 V versus the NHE.[38] From the absorption and fluorescence maxima of the mixed SRH/AA monolayer, a singlet energy (E_{00D}) of 2.29 eV can be determined. Hence the reduction potential of the excited dye ($E_{D*/D-}$) can be calculated according to eq 11, yielding a value of 1.46 V:

$$E^0_{D*/D\cdot} = E^0_{D/D\cdot} + E_{00D} \quad (11)$$

With the knowledge of the reduction potential of the excited dye and the oxidation potential of the 2A7 multilayer, it is possible to calculate the standard free energy change ($\Delta G°$) for the charge generation process, yielding a value of −0.04 eV (Table 3):

$$\Delta G° = E^0_{A+/A} - E^0_{D*/D\cdot} \quad (12)$$

This is very close to what was found for the system studied by Verschuere, where the photosensitized injection from a *N*,*N*′-bis(ethyloctadecyl)rhodamine B (SRB) monolayer into a 2A7 monolayer, deposited on an anthracene crystal, was investigated.[39] The reduction potential of rhodamine B (−0.75 V) and the excitation energy (2.19 eV) allowed them to calculate a value of eV for $\Delta G°$. For the latter system, the quantum yield is 1.8% at 1.0×10^5 V/cm for a coverage of 10%. For the photosensitized injection from oxacarbocyanine into a 2A7 monolayer, deposited on an anthracene crystal, $\Delta G°$ and ϕ_{SHC} are −0.03 eV and 0.04 at 1.0×10^5 V/cm, respectively.[28] In the present system, because the electron transfer is not assisted by the applied field, we can expect a lower quantum yield for the electron transfer. If the results of Verschuere obtained at 1.0×10^5 V/cm for a coverage of 10% are extrapolated to low

field, the quantum yield is about 1.2%, which is about 3 times larger than the value we obtained. Taking into account that, for the system investigated, the initial electron transfer step is not assisted by the electrical field, our results correspond well to the results obtained by Verschuere. This implies that the quantum yield for the SHC is mainly determined by the primary electron-transfer step and that a large fraction of injected holes reaches the opposite electrode. The low values for the quantum yield are due to the efficient competition between radiative and nonradiative decay of the excited dye and the slow charge transfer over 10 Å.[28] The relatively large tunneling distance will lead to a rather low efficiency for the charge transfer and, hence, a low quantum yield.

Recombination Mechanism. After the injection of a hole in the valence band of the 2A7 chromophore, a reduced dye molecule is left. This reduced dye molecule can be oxidized by the recombination with a hole in the valence band. From a kinetic point of view, three different types of recombination can be considered:[40] (a) geminate recombination, the injected hole oxidizes the parent reduced dye molecule; (b) alien recombination: the injected hole recombines with an impurity or a physical defect in the multilayer assembly; (c) nongeminate recombination, the injected hole oxidizes a nonparent reduced dye molecule.

The linear dependence of the photocurrent on the light intensity excludes nongeminate recombination for the range of light intensities used in the present investigation. This behavior is different from what was observed for the intrinsic in-plane photoconductivity of 2A7. However, when comparing the intensity dependence of the photocurrents obtained upon excitation of the dye (530 nm) to those obtained upon excitation of the anthracene chromophores (400 nm), one should take into account that latter are considerably smaller. As this corresponds to a smaller charge carrier density, the relative importance of non-geminate recombination will be decreased significantly. Since the excited dye molecules extract electrons from the anthracene chromophores, the resulting positive and negative charge carriers will not be in the same layer, reducing the probability of nongeminate recombination. For anthracene crystals covered with a dilute dye solution, nongeminate recombination also remains an unimportant pathway, even at high dye coverages.[27,28]

Geminate recombination will compete with the escape of the injected hole from the site where it is created. The latter process will be enhanced by increasing the applied field. This explains the initial increase of the SHC and the saturation at fields exceeding 20 kV/cm where the escape becomes much faster than geminate recombination. However, the saturation is not complete and a further, although weaker, increase of the photocurrent is observed. This is probably due to an increase of the Schubweg of the injected carriers. Contrary to the results of Verschuere et al.,[51] it cannot be attributed to an enhancement of the rate constant for the initial charge transfer. While in the system investigated by Verschuere the applied field was parallel to the direction of the initial charge transfer, it is in the systems investigated here perpendicular to that direction. Another possible way to explain the further increase of the photocurrent is that the escape of the injected hole is a two-step exchange process, of which the first step shows a rather shallow dependence upon the applied field, while the second step strongly depends on the applied field. Such a mechanism has been invoked by Eichhorn to rationalize the field dependence of the transient photocurrents observed for anthracene covered by rhodamine B.[41]

Influence of the Dye Concentration. A decrease of the quantum yield of the photosensitized photocurrent was observed when the mixing ratio between SRH and AA was increased. Also the features of the current−voltage plot depend on the concentration of the dye. This phenomenon has also been observed for photoinjection of holes from adsorbed cationic dyes into anthracene crystals,[42] for which it was attributed mainly to alien recombination of the injected holes at dye dimers and partly to energy transfer to dimers which have a lower efficiency for hole injection.[43,44] The fluorescence decays and the quantum yields, obtained for for LB-films containing *N*,*N*-bis(ethyloctadecyl)rhodamine B (SRB), suggest the formation of dimers and larger aggregates of SRB upon increasing the amount of dye.[51,57,58] However, this aggregation does not lead to a shift of the absorption or emission spectrum. This was attributed to the formation of dimers in the LB monolayer, where the transition dipoles and the vector linking the centers of the molecules form an angle of 55°. For SRH the formation of the same type of dimers can be expected.

Nongeminate recombination at dye monomers or dimers cannot be responsible for the difference between the quantum yields of the 1% and the 10% samples, since this process is borne out by the intensity effect on the photosensitized photocurrent. The distance between the dye monomers as well as between dye monomers and dimers decreases when the amount of dye increases. This can lead to an important increase in Förster energy transfer,[47] since this process depends on the sixth power of the distance. Energy transfer, which will be more efficient for the 10% sample, will lead to a decrease of the SRH sensitized photocurrent in 2A7 multilayers, since the aggregates have a less sensitizing efficiency compared to the monomers.[27,28]

Influence of Air. The photosensitized photocurrent increases when air is present in the compartment. This cannot be explained by reduction of the nongeminate recombination, since it has been shown (vide supra) that this process is not important when the 2A7 multilayer is covered with a SRH monolayer. The increase of the photosensitized photocurrent in the presence of air can be due to supersensitization, a phenomenon where the sensitizing efficiency of the dye is increased in the presence of another compound, which does not absorb in the spectral region of the dye absorption.[48] In the absence of oxygen, photosensitization will probably lead to dye consumption. The dye concentration will decrease gradually, because the radical anions formed are no longer available for photoinduced hole injection. Furthermore, they can degrade or quench the excited state of other dye molecules. The influence of an oxidant (O_2) on the steady-state sensitized hole current can arise from different oxidation reactions, which are linked with different mechanisms of sensitized hole generation: (a) Regeneration of the reduced sensitizer by oxygen after an electron has been transferred from the 2A7 chromophore to the excited sensitizer.

$$D^{-\bullet} + O_2 \rightarrow D + O_2^{-\bullet} \tag{13}$$

(b) Oxidation of the sensitizer when an electron is transferred from the excited sensitizer onto the oxidant. The oxidized sensitizer can subsequently extract an electron from the 2A7 chromophore in the ground state.

$$D^* + O_2 \rightarrow D^{+\bullet} + O_2^{-\bullet} \tag{14}$$

$$D^{+\bullet} + A \rightarrow D + A^{+\bullet} \tag{15}$$

Although $D^{+\bullet}$ is a less effective oxidant than D* (E_0 is 1.25 and 1.46 V, respectively[50]), one has to take into account that

the lifetime of D* is much shorter than that of $D^{+\bullet}$ ($\leq$ 3 ns[57] and μs-ms, respectively).

Additional experiments are necessary to distinguish between the different mechanisms and to further clarify the regeneration process of the reduced dye molecule.

At reduced pressure, the saturation behavior of the current−voltage plots could partially be attributed to consumption of dye molecules. However, taking into account the values of the photocurrent and the duration of an experiment (300 s), complete consumption of dye molecules during a voltage scan is not very likely. Furthermore, if this consumption would occur, the photocurrents measured during the second cycle would have been much smaller.

4.2.2. Excitation at $\lambda \leq$ 400 nm. Mechanism of Photosensitized Charge Generation. In agreement with in-plane conductivity in a 2A7 multilayer without a dye monolayer, the wavelength dependence of the quantum yield in the range below 400 nm suggests direct band gap excitation of the 2A7 in the double layer system. It is clear, however, from the comparison of the quantum yields, that an additional dye monolayer on top of the 2A7 multilayer increases the quantum yield of the photocurrent obtained upon excitation of the 2A7 chromophore. This phenomenon has also been observed when anthracene crystals, covered with an aqueous rhodamine B solution, were excited.[49] For the latter system, energy transfer from the first excited singlet state of the crystal to the first excited singlet state of the sensitizer rhodamine B, followed by electron transfer from the crystal to the excited sensitizer, was suggested as the mechanism of sensitized hole generation.

To check if energy transfer (eq 18) takes place before charge separation, photosensitized fluorescence (eq 19) was studied. Upon excitation of the 2A7 chromophore (eq 16), some SRH fluorescence is produced by host sensitization, which shows the occurrence of energy transfer. After energy transfer the resulting excited dye monomer can undergo the same processes as described earlier (4.2.1.). However, the 2A7 fluorescence (eq 17) still dominates and is only slightly quenched, indicating that the primary energy transfer step is not very efficient in the present device. Hence, the increase of the quantum yield cannot be attributed to energy transfer to SRH.

$$D + A \xrightarrow{h\nu} D + {}^1A^* \qquad \text{excitation at } \lambda \leq 400 \text{ nm} \qquad (16)$$

$${}^1A^* \rightarrow A + h\nu_A \qquad \text{fluorescence} \qquad (17)$$

$${}^1A^* + D \rightarrow A + {}^1D^* \qquad \text{energy transfer} \qquad (18)$$

$${}^1D^* \rightarrow D + h\nu_D \qquad \text{photosensitized fluorescence} \qquad (19)$$

Upon excitation of the anthracene chromophore, the dye molecules in the ground state can also act as primary electron acceptors (eq 20). In this case, an electron is transferred from the LUMO of the excited anthracene chromophore to the LUMO of the dye, resulting in the formation of a hole in the valence band of 2A7 and a reduced dye molecule (eq 21).

$${}^1A^* + D \rightarrow A^{+\bullet} + D^{-\bullet} \qquad \text{charge transfer quenching} \qquad (20)$$

$$A^{+\bullet} + D^{-\bullet} \rightarrow D^{-\bullet} + A + h^{+\bullet} \qquad \text{field-assisted charge separation} \qquad (21)$$

The reduction potential of SRH and oxidation potential of 2A7 are −0.92 V[50] and 1.42 V,[28] respectively. The singlet energy of 2A7 (E_{00A}) was determined to be 2.79 eV. Hence, the oxidation potential of the excited anthracene ($E_{A+/A*}$) can be calculated according to eq 22, yielding a value of −1.37 V.

$$E^0_{A^+/A^*} = E^0_{A^+/A} - E_{00A} \qquad (22)$$

This yields a value for $\Delta G°$ of −0.45 V, which means that the reaction is exothermic and energetically feasible. This process requires, however, that energy is transferred efficiently from the lower 2A7 layers to the uppermost 2A7 layer, which is probably not an efficient proces, as shown by the sensitized fluorescence experiments.

Recombination Mechanism. In contrast to what was observed when the sample was excited at 530 nm, upon excitation at 400 nm nongeminate recombination cannot completely be neglected. In comparison with the system without a dye monolayer, upon excitation at 400 nm nongeminate recombination is apparently less important. This could shed some light on the role of the dye on the increase of the photocurrent. Upon excitation of 2A7, exciton dissociation will lead to mobile electrons and holes. When the former are captured by the SRH molecules, the electrons and holes will be separated in space and the efficiency of recombination will be decreased. Furthermore, it is possible that the dye molecules will capture the electrons from the geminate electron−hole pairs formed upon excitation of 2A7 and in this way increase the photocurrent further.

5. Conclusions

In this contribution, it was shown that high quality multilayer films of the amphiphilic long-chain derivative of anthracene 2A7, which resemble structurally the ab-plane of anthracene crystals, allow the observation of in-plane photoconduction. Using an amphiphilic rhodamine derivative (SRH), it is possible to create a double layer system where the dye monolayer and the 2A7 multilayer are the charge generation layer and the charge transport layer, respectively. Both upon excitation of the dye chromophore or the anthracene chromophore, the dye acts as the primary electron acceptor, leading to the generation of mobile holes. The quantum yields and the effects of several experimental parameters are in agreement with results obtained for anthracene single crystals. This suggests that the same mechanisms are operative for the intrinsic as well as for the sensitized photocurrents.

Acknowledgment. M.V.d.A. is a "Onderzoeksleider" of the "Fonds voor Wetenschappelijk Onderzoek-Vlaanderen" (F.W.O.). A.V. thanks the I.W.T. and the K. U. Leuven for financial support. The authors thank the Belgian Ministry of Science Programmation through IUAP IV-11, F.W.O., and the "Nationale Loterij: for financial support.

References and Notes

(1) E-mail: mark.vanderauweraer@mds.kuleuven.ac.be.
(2) Mulder, B. J. *Philips Res. Rep., Suppl.* **1968**, *4*, 1.
(3) Petelenz, P.; Mucha, D. *Chem. Phys.* **1991**, *154*, 145.
(4) Gerischer, H.; Willig, F. *Top. Curr. Chem.* **1976**, *61*, 31.
(5) Killesreiter, H. *Ber. Bunsen-Ges. Phys. Chem.* **1978**, *82*, 503.
(6) Willig, F.; Michel-Beyerle, E. *Photochem. Photobiol.* **1972**, *16*, 371.
(7) Willig, F.; Gerisher, H. *Top. Curr. Chem.* **1976**, *61*, 331.
(8) Jones, R.; Tredgold, R. H.; O'Mullane, J. E. *Photochem. Photobiol.* **1980**, *32*, 223.
(9) Kuhn, H. *Pure Appl. Chem.* **1979**, *51*, 341.
(10) Donovan, K. J.; Sudiwala, R. V.; Wilson, E. G. *Mol. Cryst. Liq. Cryst.* **1991**, *194*, 337.
(11) Donovan, K. J.; Sudiwala, R. V.; Wilson, E. G. *Thin Solid Films* **1992**, *210/211*, 271.

(12) Roberts, G. G.; McGinnity, M.; Barlow, W. A.; Vincett, P. S. *Thin Solid Films* **1980**, *223*.
(13) Sugi, M.; Fukui, T., Iizima, S.; Iriyama, K. *Bull. Electrotech. Lab.* **1979**, *43*, 625.
(14) Sugi, M.; Saito, M.; Fukui, T.; Iizima, S. *Thin Solid Films* **1983**, *99*, 17.
(15) Durfee, W. S.; Storck, W.; Willig, F.; von Frieling, M. *J. Am. Chem. Soc*. **1987**, *109*, 1297.
(16) Van der Auweraer, M.; Willig, F. *Isr. J. Chem*. **1985**, *25*, 274.
(17) Itaya, A.; Van der Auweraer, M.; Verschuere, B.; De Schryver, F. C. *Isr. J. Chem*. **1991**, *31*, 169.
(18) Kaplun, A. P.; Basharuli, V. A.; Shchukina, L. G.; Svhets, V. I. *Bioorg. Khim.* **1979**, *5*, 1826.
(19) Ioffe, I. S.; Shapiro, A. L. *Zh. Org. Khim.* **1970**, *6*, 2, 369.
(20) Biesmans, G.; Verbeek, G.; Verschuere, B.; Van der Auweraer, M.; De Schryver, F. C. *Thin Solid Films* **1989**, *169*, 127.
(21) Meier, M. In *Organic Semiconductors*; Verlag Chemie: Weinheim, 1974; p 88.
(22) Catry, C.; Van der Auweraer, M.; De Schryver, F. C.; Bengs, H.; Häussling, L.; Karthaus, O.; Ringsdorf, H. *Makromol. Chem*. **1993**, *194*, 2985.
(23) Gemma, A.; Mizushima, K.; Miura, A.; Azuma, M. *Synth. Met.* **1987**, *809*, 809.
(24) Biesmans, G.; Van der Auweraer, M.; De Schryver, F. C. *Langmuir* **1990**, *6*, 277.
(25) Verschuere, B.; Van der Auweraer, M.; De Schryver, F. C. *Thin Solid Films* **1994**, *244*, 995.
(26) Biesmans, G.; Van der Auweraer, M.; Catry, C.; Meerschaut, D.; De Schryver, F. C.; Storck, W.; Willig, F. *J. Phys. Chem.* **1991**, *95*, 3771.
(27) Schieler, L.; Nichols, P. L. *J. Electrochem. Soc*. **1956**, *106*, 60.
(28) Baker, S.; Petty M. C., Roberts G. G.; Twigg, M. V. *Thin Solid Films* **1983**, *99*, 53.
(29) Itaya, A.; Okamoto, K. I.; Kusabayashi, S. *Bull. Chem. Soc. Jpn*. **1979**, *52*, 2218.
(30) Van der Auweraer, M.; Catry, C.; De Schryver F. C.; Bengs, H.; Karthaus, O.; Häussling, L.; Ringsdorf, H. In *Spectroscopy and Chemistry in Small Domains*; Masuhara, H., Ed.; Elsevier Science B. V.: Amsterdam, 1994; p 455.
(31) Mort, J.; Pai, D. M. In *Photoconductivity and related phenomena*; Elsevier: Amsterdam, 1976.
(32) Chance, R. R.; Braun, C. L. *J. Chem. Phys.* **1976**, *64*, 9, 3573.
(33) Lyons, L. E.; Milne, K. A. *J. Chem. Phys*. **1976**, *65*, 4, 1474.
(34) Onsager, L. *Phys. Rev*. **1938**, *54*, 554.
(35) Kearns, D. R. *J. Chem. Phys*. **1966**, *45*, 3966.
(36) Vaubel, G.; Bässler, H. *Phys. Status Solidi* **1968**, *26*, 599.
(37) Nickel, B. *Mol. Cryst. Liq. Cryst.* **1972**, *18*, 227.
(38) Biesmans, G. Ph.D. Thesis, Katholieke Universiteit, Leuven, Belgium, 1989.
(39) Verschuere, B.; Van der Auweraer, M.; De Schryver, F. C. *Chem. Phys*. **1991**, *149*, 385.
(40) Biesmans, G.; Van der Auweraer, M.; Catry, C.; De Schryver, F. C.; Yonezawa, Y.; Sato, T. *Chem. Phys*. **1992**, *160*, 97.
(41) Eichhorn, M.; Willig, F.; Charlé, K. P.; Bitterling, K. *J. Chem. Phys*. **1982**, *76*, 4648.
(42) Willig, F. *Chem. Phys. Lett*. **1976**, *40*, 331.
(43) Kemnitz, K.; Murao, T.; Yamasakin, I.; Nakashima, N.; Yoshihara, K. *Chem. Phys. Lett*. **1983**, *101*, 337.
(44) Nakashima, N.; Yoshihara, K.; Willig, F. *J. Chem. Phys*. **1979**, *73*, 3553.
(45) Van der Auweraer, M.; Verschuere, B.; De Schryver, F. C. *Langmuir* **1988**, *4*, 583.
(46) Nakashima, N.; Yoshihara, K.; Willig, F. *J. Phys. Chem.* **1980**, *73*, 3553.
(47) Förster, T. *Discuss. Faraday Soc*. **1959**, *27*, 7.
(48) Möbius, D. In *Light-Induced Charge Separation in Biology and Chemistry*; Proceedings Dahlem Konferenzen, Gerischer, H., Katz, J. J., Eds.; Verlag Chemie: New York, 1979; pp 171−185.
(49) Mulder, B. J.; De Jonge, J. *Proc. K. Ned. Akad. Wet*. **1963**, *B66*, 303.